doi.org/10.36721/PJPS.2021.34.1.SUP.283-290.1

Effectuation of loading a natural acetyl carnosine derivative within a promising cross-linked cyclodextrin spongey-like nanospheres on Physicochemical characterization and release behavior

Alia Badawi[1], Magdy Mohammed[1], Rawia Khalil[2], Ruddy Ali[3] and Sally Abou Taleb[2]*

[1]Department of Pharmaceutics, Faculty of Pharmacy, Cairo University, Cairo, Egypt
[2]Department of Pharmaceutical Technology, National Research Centre, Dokki, Giza, Egypt
[3]Faculty of Pharmacy, 6 October University, Cairo, Egypt

Abstract: This study centered on the ability of the cross-linked nano-sponge system to load the drug and to improve its physicochemical and dissolution properties. A spectrophotometric method was used to determine the wavelength of maximum absorbance of the drug. The ultrasonic-assisted synthesis method was used for nano-sponge preparation. Solution-state interactions, encapsulation efficiency and production yield, and *in-vitro* release were also investigated. Nano-sponges were characterized by Transmission Electron-Microscopy (TEM), Scanning Electron-Microscopy (SEM), Fourier Transform-Infrared Spectroscopy (FT-IR), Differential Scanning Calorimetry (DSC), and X-Ray Diffractometry (X-RD) studies. The maximum absorption wavelength of N-acetyl–L-carnosine was found to be at 210 nm. Solution-state interaction studies revealed a bathochromic shift. The production yield of nano-sponges ranged from 59.58% to 72.54%. In-vitro release study showed a sustained drug release for 228 hours. TEM images showed regular spherical shapes and sizes of nano-sponges. Their average particle size ranged from 28 nm to 79.2 nm. DSC data documented the drug-polymer interactions. FT-IR determined the presence of functional groups. X-RD showed the physicochemical characteristics of nano-sponges. Proving successful development of N-acetyl–L-carnosine polymeric nano-sponge system with a suitable drug delivery over an extended period beside a noticeable improvement in the physicochemical characterization.

Keywords: Nano-sponge, hydroxy-propyl-β-cyclodextrin, N-acetyl–L-carnosine, ultrasonic technique release.

INTRODUCTION

Carnosine (β-alanyl-L-histidine) was well defined at the beginning of the 20th century (Oppermann *et al*., 2019). Such carnosine enantiomer (L-carnosine) is considered as a bio-active natural di-peptide responsible for metabolism regulation and found in many mammalian tissues. Also, the L-carnosine had a powerful activity as a natural antioxidant (Babizhayev *et al*., 1994). In addition, to its ability to be cleared through the urine or decomposed by a certain enzyme (carnosinase) presented in the blood plasma, kidney, liver, and other tissues and thus not aggregated in the tissues (Babizhayev *et al*., 1994). The N-acetyl-L-carnosine (NAC) derivatives also exist within the skeletal mammalian muscle (O'Dowd *et al*., 1988). The naturally occurring NAC is identified as; the pro-drug of L-carnosine. It is characterized by its resistance to the enzymatic hydrolyzation by carnosinase serum enzyme, which prolongs its physiological responses (Babizhayev *et al*., 1996). On the other hand, such resistance may also negatively affect NAC activity and clearance (Babizhayev *et al*., 1996).

Nano-sponge is a novel type of hyper cross-linked polymers (Trotta *et al*., 2012). Nano-sponge tiny mesh-like structure enhances stability, reduces side effects and modifies drug release (Allahyari *et al*., 2019). Moreover, it's typically porous outer surface, permits a sustained release of the drug (Ahmed *et al*., 2013). Also, such nano-tiny-spongy structures move within the body till they achieve a specific target spot and stick to its surface, and then start to release the drug moieties in a controllable pattern (News.vanderbilt.edu Available online, 2010). In addition, they intend to encapsulate various compounds improving their ability to transport through aqueous media (Tejashri *et al*., 2013).

The hydroxy-propyl-β-cyclodextrin (HP*β*-CD) nano-sponge system type was found to consist of; a freeze-dried sponge-like structure with a favorable high ability to interact with tiny elements in their matrixes (Torne *et al*., 2013). Such type of nano-sponge can be obtained by cross-linking many classes of cyclodextrin using definite cross-linkers (Ansari *et al*., 2011; Torne *et al*., 2013) as diphenyl carbonate (DPC) (Abou Taleb *et al*., 2020), leading to a nano-sponge system with high solubilizing efficiency for hydrophobic drugs (Cavalli *et al*., 2006; Swaminathan *et al*., 2007) and with the capability to formulate either inclusion or/and non-inclusion complexations with many drug molecules (Swaminathan *et al*., 2010). This sort of advantageous nano-sponge can protect unstable drug molecules and creates several and

**Corresponding authors:* e-mails: aboutaleb2012@gmail.com, l_ully_85@hotmail.com

different routes of administration for drug delivery. Beta-cyclodextrin (*β*-CD) derivative polymers appear to be the most widely used attractive alternative among all naturally occurring polysaccharides, due to their low cost and high biodegradability and biocompatibility (Tejashri *et al*., 2013), which make them easily cleared with no concerning of any un-wanted aggregations to occur within the body tissues.

Hence, such study aim was seeking to develop and characterize cyclodextrins-based NAC nano-sponge to improve its physicochemical and dissolution properties in order to achieve a successfully loaded NAC nano-sponge system with a sustainable release and proper encapsulation, yield and physicochemical characteristics that can grant it further attention as a suitable formulation for pharmaceutical interests.

MATERIALS AND METHODS

Materials

NAC was obtained from SEIDC, Shanghai Industries Cooperation, [China]. HP*β*-CD (KLEPTOSE, MW=1380) was given kindly by Roquette Co. [France]. Diphenyl-carbonate was bought from AOC, Acros Organic Co. [Belgium]. Anhydrous disodium hydrogen-phosphate and Potassium dihydrogen-phosphate were purchased from GPC, El-Gomhuoria Pharmaceutical Chemical, [Egypt].

Methods

Calibration curve estimation of NAC

Specified concentrations of NAC in phosphate buffer (pH 7.4) solutions were scanned spectrophotometrically between 200 and 400nm in order to define the maximum-absorbance wavelength (λmax). The standard curve was also plotted.

Preparation of HPβ-CD nano-sponge

Nano-sponge was prepared using the Ultrasound-Assisted synthesis method (Trotta *et al*., 2007). DPC was used as a cross-linker and mixed with HP*β*-CD in specific molar-ratios of; [(HP*β*-CD: DPC) were 1:0.5, 1:1, 1:2, 1:4, 2:1 and 4:1], then such mixture was exposed to sonication and heated up to 90° C. And then the yielded product was washed off with distilled-water, in order to eliminate non-reacted polymer. The final product was desiccated under vacuum and kept at 25°C (Swaminathan *et al*., 2010; Trotta *et al*., 2007).

Loading NAC in HPβ-CD nano-sponge

Preparation of NAC-loaded nano-sponges was fulfilled by a technique called freeze-drying (lyophilization). Excess amount of NAC was added to accurately weighed quantities of nano-sponges and sonicated for 20 mins and then stirred for 24 hrs. The outcome suspensions were allowed to centrifuge for 15mins at 9,000 rpm. The supernatant was finally lyophilized at, -20°C: 960mT, to achieve the drug-loaded nano-sponge (Torne *et al*., 2013; Trotta *et al*., 2007).

Preparation of NAC- HPβ-CD complex

The preparation of such complexes was carried out by obeying the kneading method (Ammar *et al*., 2013). A physical mixture of NAC and HP*β*-CD was wetted till a paste was made. Such paste was then kneaded for 15 mins followed by drying it under vacuum at room temperature.

Solution state interaction studies

Increasing concentrations of both, parent polymer HP*β*-CD and of the formulated nano-sponge solutions (2-10 mM/L) respectively were mixed with a defined amount of the drug (10 mg). The samples were then kept over-night. Then samples were scanned at their λ max and the absorbance was measured. The parameter studied was represented by, the spectral band shift for both the HP*β*-CD drug complex and the formulated nano-sponge (Terekhova and Obukhova, 2007).

Drug content

Nano-sponges' containing precisely weighed quantity of the drug were measured spectrophotometrically. Estimation of drug content of all ratios was done using the following expressions:

drug content = (S_{act} / S_{the}) X 100

Where S_{act} = actual drug content within the nano-sponge measured quantity, and S_{the} = theoretical drug content within the nano-sponge (Abou Taleb *et al*., 2020).

Production yield

The production yield value was calculated as follows (Furniss, 1989). Production yield % = Weight of dry nano-sponges ×100/ Total solids weights

In-vitro release of NAC nano-sponges

The *in-vitro* release study on the blank and NAC loaded nano-sponge ratios was done in triplicates in phosphate buffer (pH=7.4), using a cellulose dialysis-membrane, with a cut off 12,000 Dalton, at 37±1°C under 100 rpm rotation for 288 hours continuously. Samples were withdrawn at pre-determined intervals with maintaining sink condition and analyzed spectrophotometrically (Torne *et al*., 2013; Penjuri *et al*., 2016).

Characterization of nano-sponge

TEM

TEM morphology investigation of nano-sponges was observed using a transmission electron microscope (Philips CM 10). Measuring the particle size was carried out with the NIH-image software (Tejashri *et al*., 2013).

SEM

SEM involves imparting surface topography and morphology, using LEO 440i-UK scanning electron microscope (Tejashri *et al*., 2013).

Particle size of nano-sponges

Nano-sponges particle size was measured by, PSS, Santa Barbara, USA, Dynamic light scattering instrument using a HeNe laser 632 nm line, as the incident light, with an angle of 90° at 25°C. The average particle size was expressed and the polydispersity index was also estimated (Torne *et al*., 2013).

FT-IR

Infrared spectra were recorded by FT-IR Shimadzu 8400S spectrophotometer (Japan) following the KBr-pellet method (Branham *et al*., 2011). Individual NAC and *β*-cyclodextrins were employed as controls. Samples spectra were obtained by placing them in the light pathway using a resolution of 16 cm^{-1} and a scanning range of 4,000 - 500 cm^{-1} (Sinha *et al*., 2010).

DSC

DSC thermograms were determined using Mettler-Toledo 821e (Switzerland) differential scanning calorimeter provided with an Inter-cooler. One mg of the samples was heated in a well plugged aluminum pan at a heating rate of 10 °C min-1, under a nitrogen-flow of ten ml min-1, over a temperature ranging from 20 to 450°C (Tejashri *et al*., 2013). Indium was used to calibrate both of heat flow and temperature.

X-RD

X-ray diffraction pattern was studied by using Siemens D5000 (Germany) X-ray diffractometer. Dried sample was Ni-filtered and irradiated with Cu-k-α-radiation, at 40 mA current and 45 kilo-voltages, using a scanning rate of 2 min^{-1}, over a diffraction angle (2θ) ranging between 4–50 ° (Ammar *et al*., 2013).

STATISTICAL ANALYSIS

Were displayed as mean ± SD (n=3). The group comparison variance evaluation was achieved by (One Way-ANOVA) followed by LSD-test and computed using the SPSS® software. Differences were stated significant when ($p<0.05$).

RESULTS

NAC Calibration and Standard curve

The λmax of NAC in phosphate buffer at pH=7.4 was found to be at 210 nm. The standard curve for NAC revealed a perfect linear relationship between the absorbance values at 210 nm and different serial drug concentrations (fig. 1), proved also by the coefficient value (R^2) that was almost 1, indicating a fairly high linearity relationship.

Solution state interaction

Fig. 2 clearly represented the influence of the gradual increase of both HP*β*-CD concentration and nano-sponge concentration in the spectrum of NAC. And it was noticed, that the gradual increase in nano-sponge concentration from 2 to 10mM, comparatively to that of NAC- HP*β*-CD complex solution concentration, caused noticeable changes jointly in; the maximum absorbance with a noticeable bathochromic shift of NAC beside the absence of the previously mentioned bands, compared to the complex effect of HP*β*-CD solution alone.

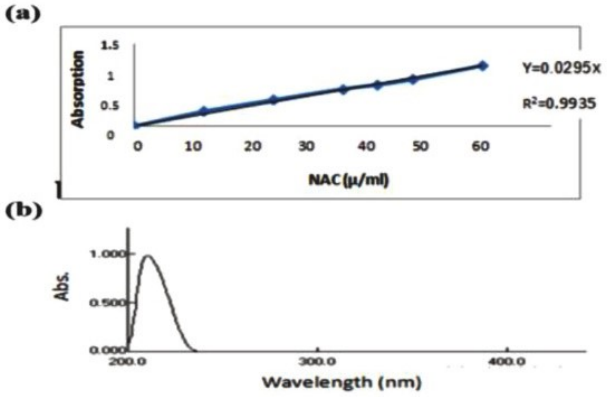

Fig. 1: (a) Standard curve of NAC in pH 7.4 at 210 nm and (b) UV spectrum of NAC in pH 7.4

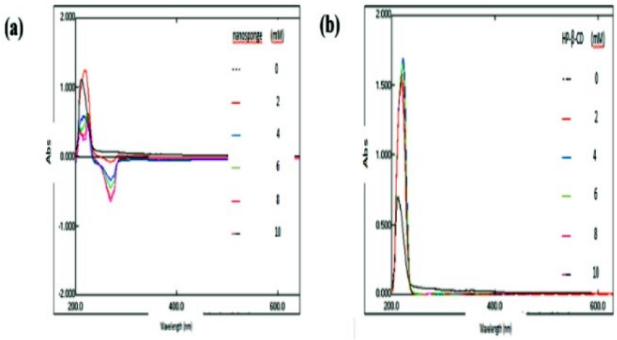

Fig. 2: Differential ultraviolet absorption spectrum of NAC in presence of: (a) HP*β*-CD (b) Formulated nano-sponge

Table 1: Drug content and production yield of different ratios of NAC loaded nano-sponges.

HP*β*-CD: DPC	Drug content (%) ±SD[a*]	Production Yield (%) ±SD[a*]
1:0.5	87.32±0.01	64.75±0.01
1:1	106.11±0.03	72.54±0.03
1:2	75.08±0.20	70.39±0.03
1:4	78.68±0.02	60.87±0.40
2:1	59.98±0.01	59.98±0.02
4:1	64.38±0.01	59.58±0.01

[a*]Data are expressed as Mean ± SD, n=3

Drug Content data

As demonstrated in table 1, drug content percentage among formulated nano-sponges was found to be the best

(106.11%) for the equimolar ratio of HP*β*-CD: DPC (1:1). Otherwise, with further increase in the polymer or in cross-linker concentration, drug content percentage was found to be increased; as for the polymer it increased from 59.98% (ratio 2:1) to 64.38% (ratio 4:1), respectively and for the cross-linker it increased from 75.08% (ratio 1:2) to 78.68% (ratio 1:4), respectively.

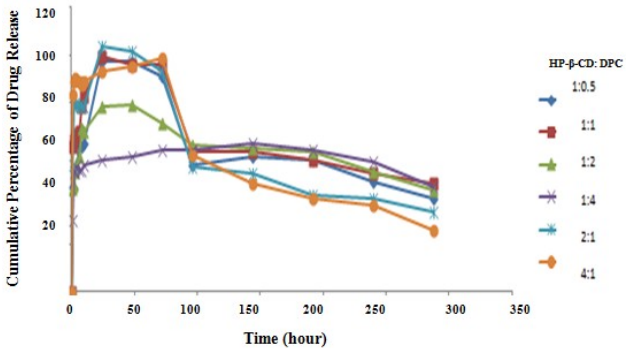

Fig. 3: *In vitro* release study of nano-sponge formula were insignificant different from each other's ($p>0.05$) using ONE Way-ANOVA

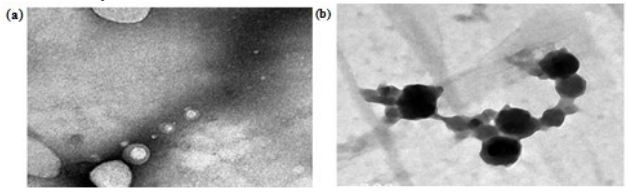

Fig. 4: TEM of: (a) blank nano-sponge and (b) NAC loaded nano-sponge

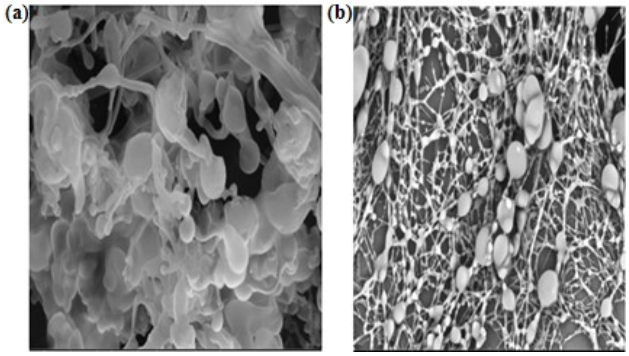

Fig. 5: SEM of: (a) blank nano-sponge and (b) NAC loaded nano-sponge

Table 2: Particle size and polydispersity index (PDI) of different ratios for NAC loaded nano-sponges

HP*β*-CD: DPC	Drug content (%) ±SD[a*]	Production Yield (%) ±SD[a*]
1:0.5	87.32±0.01	64.75±0.01
1:1	106.11±0.03	72.54±0.03
1:2	75.08±0.20	70.39±0.03
1:4	78.68±0.02	60.87±0.40
2:1	59.98±0.01	59.98±0.02
4:1	64.38±0.01	59.58 ±0.01

[a*]Data are expressed as Mean ± SD, n=3, and [b*]PDI is the polydispersity index

Production yield data

Nano-sponges production yields were ranging between 59.58% and 72.54% (table 1). HP*β*-CD: DPC ratio was found to influence the production yield remarkably. In the state of HP*β*-CD: DPC ratio 1:1, production yield was very high, i.e., 72.54%, whilst for HP*β*-CD: DPC ratio 4:1, it was found to be 59.58%.

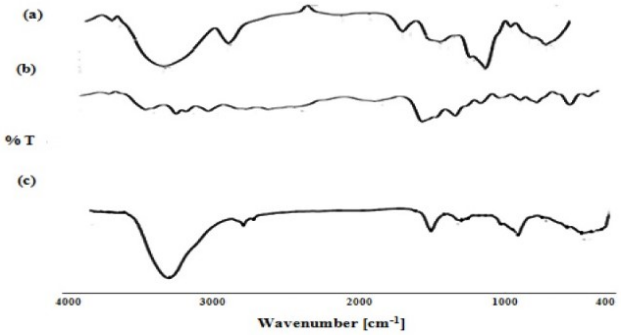

Fig. 6: FT-IR of: (a) NAC, (b) HP*β*-CD, (c) 1:1 (HP*β*-CD: DFC) nano-sponge

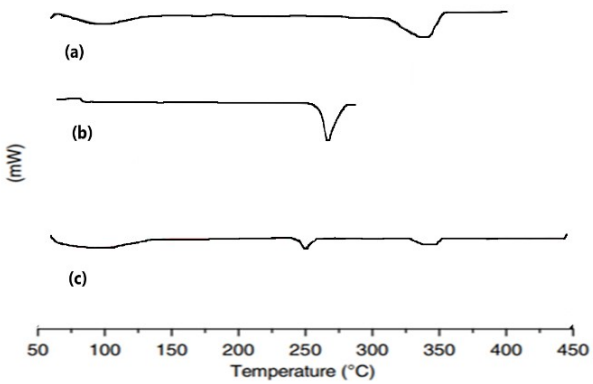

Fig. 7: DSC thermograms of: (a) HP*β*-CD, (b) NAC, (c) 1:1 (HP*β*-CD: DFC) nano-sponge

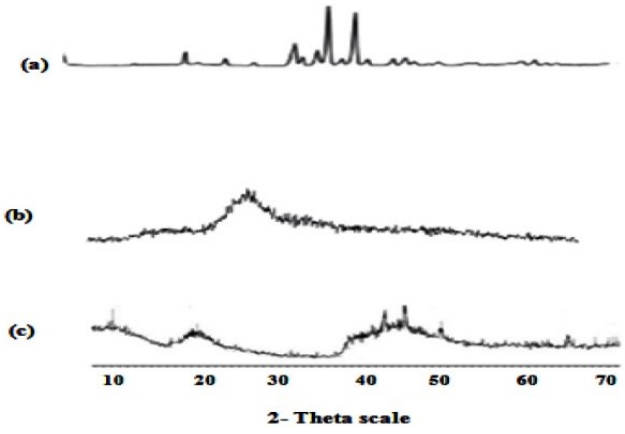

Fig. 8: X-ray diffraction patterns of: (a) NAC, (b) HP*β*-CD, (c) 1:1 (HP*β*-CD: DFC) nano-sponge

In-vitro release data of NAC nano-sponges

In-vitro release study of NAC from nano-sponge ratios, showed a sustained controlled drug release manner for

228 hours as illustrated in fig. 3. A bi-phasic release profile of NAC was recognized, including; an initial burst-phase followed by a sustained-phase pattern. Nano-sponge systems with lower cross-linker ratios reached 90 % of drug release after 48 hours. Additionally, the release rate was found to depend on the cyclodextrin to cross-linker ratios. The release rate of nano-sponges with ratios of 1:0.5, 1:1, 1:2, and 1:4, was slightly significant ($p=0.05$), while, the further increase in cyclodextrin ratios (as in 2:1 and 4:1), resulted in release rates insignificant different from each other's ($p>0.05$).

TEM

TEM images revealed that the nano-sponges lineaments were un-affected even after drug encapsulation as they showed in fig. 4 a uniform spheroidal shape and size arranged in a net-work structure.

SEM

The SEM images of the NAC nano-sponges, fig. 5, appeared as globular particles with highly pours surface tunneled inwards in a three-dimensional web structure.

Particle Size Data

The particle size analysis revealed that, the studied nano-sponges measured average particle size ranged from 28 nm to 79.2 nm as seen in table 2. The polydispersity indexes (PDI), were found to be below one (table 2), indicating such systems homogeneity.

From the previously mentioned results (solution state studies, drug content, production yield, release, particle size, and polydispersity index), as the equimolar ratio of HP*β*-CD: DPC (1:1) showed the optimistic outcome, thus it would be subjected for further estimation in this research.

FT-IR Data

As shown in fig. 6, in the region of high-frequency, NAC showed certain characteristic IR vibrational peaks including stretching vibrational bands at 3,237cm^{-1} and 3,049 cm^{-1} attributing to; the amide-hydrogen group and the terminal protonated-amine, $NH3^{+}$, of the free L-carnosine, respectively. Plus, other important peaks that revealed at 2,162cm^{-1} and 1,643cm^{-1} due to; the imidazole (N–H) group vibrational bending and the amide group stretching sequentially (Sinha *et al*., 2010). Furthermore, the IR spectra of HP*β*-CD (fig. 6-b) showed wide absorption bands at 3383, 3396, and 3402 cm-1 as a reason of; the OH-group stretching (Ansari *et al*., 2011). In formula (1:1) NAC nano-sponge FT-IR spectra (fig. 6-c), new nano-sponge sharp peaks had appeared where only few characteristic peaks of NAC were visible. Due to a marked alteration in the fingerprint region; 2505.05–3786.57 cm-1, which was masked with HP*β*-CD peaks. Also, the N-H stretching band of NAC at 2,162 cm-1 was disguised and shifted in the nano-sponge, to appear as a single broad peak.

DSC Data

In fig. 7, DSC thermo-gram of pure NAC demonstrated a sharp endo-thermic peak, the thermo-gram of pure HP*β*-CD revealed a very wide endo-thermic peak in the zone of 85.49°C. Otherwise, a decrease and shifting of the de-hydration endo-thermic peak of HP*β*-CD, as well as, in the melting peak of NAC were observed in the (1:1) NAC nano-sponge thermogram in fig. 7-c, pursued by a high decomposition exo-thermic peak beginning at 420 °C indicating a more stable (1:1) nano-sponge.

X-RD Data

The X-ray diffractogram of 1:1 nano-sponge showed a decrease in the intensity of some peak's correspondent to both NAC and HP*β*-CD, on the other hand, it was no more doable to recognize the characteristic crystallinity peaks of the free drug. In addition, many new peaks were also noticed (fig. 8-c). As seen in fig. 8-b, pure HP*β*-CD exhibited one diffraction peak.

DISCUSSION

The solution state study noticeable shift showed by the nano-sponge drug system relatively to HP*β*-CD drug-complex might be explained due to the insertion of NAC into the macrocyclic cavity that was associated with changing in its circumference parallel to the inclusion phenomena due to HP*β*-CD addition and cross-linking with nano-sponge, respectively, thus the distinct alteration in both absorbance and bathochromic shift were requisite (Spulber *et al*., 2008). NAC band disappearance indicated that portion of the NAC molecule was surrounded by cyclodextrin in the nano-sponge profile, that might reflect drug enclosure inside its cavity (Trotta *et al*., 2012; Terekhova and Obukhova, 2007). Also, the presence of various amounts of the cross-linking agent (DPC) permitted the possibility to regulate the channels between cyclodextrin molecules, thereby modulating a porous network formation and accordingly positively affecting both of the inclusion amplitude and the solubility strength of the nano-sponges (Challa *et al*., 2005).

The increased drug content with increasing polymer concentration explained as polymer increased more spaces became available to load more drug moieties. While with increasing the cross-linker the higher affinity of the cross-linked polymer to the drug in the aqueous phase elucidate their higher drug content, otherwise, the rest % of the drug lost might be referred to the dissolution of some drug in the solvent or the aqueous phase used (Ansari *et al*., 2011; Loftsson *et al*., 2005).

Production yield data reflected that, the lower the cross-linker ratio, the lower the formation of a completed net-work of the nano-sponge and thus the lower the production yield (Rao *et al*., 2013). Furthermore, the increase in production yield (72.54%) at the equimolar

HP*β*-CD: DPC (1:1) ratio, could be a reason of the abbreviated diffusion rate from the perfect nano-sponge net-work centered solution to the aqueous phase, that supplied an extra time leading to an ameliorated yield.

The *in-vitro* release initial burst-phase was probably linked to the adsorption of few drug molecules on the surfaces of the nano-sponges or their presentation as non-inclusion molecules. while, the second sustained release phase was attributed to the inclusion of NAC molecules within the nano-sponge complex (Trotta *et al*., 2012). Also, it was noticed that the hydrophobic power of the cross-linker, which retarded the NAC release from nano-sponge formulations, might be beneficial in drug release controlling. The elevated drug release percentages of nano-sponges with lower cross-linker ratios, might be related to the lower formation of totally cross-linked nano-sponges.

The SEM web structure may be due to the pervasion of the dissolvent from the nano-sponge surface (Penjuri *et al*., 2016; Tejashri *et al*., 2013). In addition, to the cross-linking effect of (DPC) that, acted like teeny grappling clasps to join various portions of the polymer together, in order to achieve spheroidal shaped particles fraught with chambers (cavities), where the drug molecules could be hoarded (Penjuri *et al*., 2016).

The narrow particle size range of these nano-sponges exemplified a unimodal particle size distribution that agrees with the size range, 10-500nm, documented for an idealistic effective cyclodextrin nano-porous system (Ahmed *et al*., 2013). The reduced particle size (28 nm) and PDI (0.396) for the ratio 1:1 could be related to the steadiness of the nano-sponge system and to the lowering of agglomeration resulting in a more homogenous nano-system (Terekhova and Obukhova, 2007).

Shifting of the nano-sponge IR peaks to different higher and lower wave-numbers in contrast to the pure NAC and HP*β*-CD, suggested a disintegration of the intermolecular hydrogen-bonds of the free drug crystal-molecules, and the establishing of a monomeric dispersion of the drug as a result of the inter-action with cyclodextrin molecules, which might be due to the drug inclusion within the cyclodextrin cavities (Sinha *et al*., 2010), indicating a distinct inter-action between the drug and nano-sponges (Trotta *et al*., 2007).

Pure NAC sharp melting DSC endotherm manifested that the drug melting point followed the decomposition of substances, also it indicated a crystalline drug nature (Trotta *et al*., 2007). Pure HP*β*-CD broad endo-thermic peak referred to the losing of water moieties in the form of; residual humidity, as well as, the water lost from the cavities, by evaporation (Kacsó *et al*., 2010). The low-intensity drug endothermic peak in 1:1 nano-sponge could be referred to the existence of some un-complexing drug (NAC) moieties in the nano-system (Trotta *et al*., 2007). The increase in the decomposition temperature, may be an evidence of the inclusion between NAC and HP*β*-CD resulting in a more stable nano-sponge system (Esclusa-Diaz *et al*., 1996; Mura *et al*., 1999).

The new peaks noticed in the X-RD of 1:1 nano-sponge, might be a shred of evidence for the formation of complexes (Tønnesen *et al*., 2002). Pure HP*β*-CD diffraction peak was referred to its extremely amorphous nature, which could explain why the nano-sponges prepared with HP*β*-CD, were higher amorphously in nature, (Blanco *et al*., 1991), compared with the free drug and HP*β*-CD molecules (Connors, 1995). That explains the nano-sponge fluffy porous powder obtained after the freeze-drying process. When the drug was in the amorphous phase, the drug molecules slowly diffused through the polymeric matrix, leading to a sustained, controlled release of the encapsulated drug (Connors, 1995). Such data explained the *in-vitro* release results within this study.

Overall, all the above outcomes were evidences for the formation of successful promising nano-carries of NAC especially for sustainable drug delivery that encourages further studying for its bioactivity.

CONCLUSION

Polymeric nano-sponge based system of NAC was developed successfully using Ultrasound-Assisted synthesis method to prolong the drug delivery period and to improve physicochemical characterization. The reported method in the present study was found to be uncomplicated, reproducible and fast; which allowed the formation of highly cancellus, spheroidal nano-sponges with a promising sustained dissolution rate of the prepared drug-polymer ratios with remarkable; drug content, production yield, and particle size. Among the all prepared NAC nano-sponges, the (1:1) formulation was chosen on the basal of its excellency in terms of; physicochemical characterization, yield, drug content, particle size and drug release. As a conclusion, it was found that HP*β*-CD based nano-sponges could be used as a potentially active nano-carrier for the NAC delivery.

REFERENCES

Abou Taleb S, Badawy Darwish A, Abood A and Mohamed AM (2020). Investigation of a new horizon antifungal activity with enhancing the antimicrobial efficacy of ciprofloxacin and its binary mixture via their encapsulation in nanoassemblies: *in vitro* and *in vivo* evaluation. *Drug Dev. Res.*, **81**(3): 347-388.

Ahmed RZ, Patil G and Zaheer Z (2013). Nanosponges-a completely new nano-horizon: Pharmaceutical

applications and recent advances. *Drug Dev. Ind. Pharm.,* **39**(9): 1263-1272.

Allahyari S, Trotta F, Valizadeh H, Jelvehgari M and Zakeri-Milani P (2019). Cyclodextrin-based nanosponges as promising carriers for active agents. *Expert Opin. Drug Deliv.*, **16**(5): 467-479.

Ammar H, Ghorab M, Mostafa D, Makram T and Ali R (2013). Host–guest system of etodolac in native and modified β-cyclodextrins: Preparation and physicochemical characterization. *J. Incl. Phenom. Macrocycl. Chem.,* **77**(1-4): 121-134.

Ansari KA, Vavia PR, Trotta F and Cavalli R (2011). Cyclodextrin-based nanosponges for delivery of resveratrol: in vitro characterisation, stability, cytotoxicity and permeation study. *AAPS Pharm. Sci. Tech.,* **12**(1): 279-286.

Babizhayev MA, Seguin M, Gueyne J, Evstigneeva R, Ageyeva E and Zheltukhina G (1994). L-Carnosine (β-alanyl-L-histidine) and carcinine (β-alanylhistamine) act as natural antioxidants with hydroxyl-radical-scavenging and lipid-peroxidase activities. *Biochem. J.,* **304**(2): 509-516.

Babizhayev MA, Yermakova VN, Sakina NL, Evstigneeva RP, Rozhkova EA and Zheltukhina GA. (1996). Nα-Acetylcarnosine is a prodrug of L-carnosine in ophthalmic application as antioxidant. *Clin. Chim. Acta,* **254**(1): 1-21.

Blanco J, Vila-jato JL, Otero F and Anguiano S (1991). Influence of method of preparation on inclusion complexes of naproxen with different cyclodextrins. *Drug Dev. Ind. Pharm.,* **17**(7): 943-957.

Branham ML, Singh P, Bisetty K, Sabela M and Govender T (2011). Preparation, spectrochemical, and computational analysis of L-carnosine (2-[(3-aminopropanoyl) amino]-3-(1H-imidazol-5-yl) propanoic acid) and its ruthenium (II) coordination complexes in aqueous solution. *Molecules,* **16**(12): 10269-10291.

Cavalli R, Trotta F and Tumiatti W (2006). Cyclodextrin-based nanosponges for drug delivery. *J. Incl. Phenom. Macrocycl. Chem.,* **56**(1-2): 209-213.

Challa R, Ahuja A, Ali J and Khar R (2005). Cyclodextrins in drug delivery: An updated review. *AAPS Pharm. Sci. Tech.,* **6**(2): E329-E357.

Connors KA. (1995). Population characteristics of cyclodextrin complex stabilities in aqueous solution. *J. Pharm. Sci.,* **84**(7): 843-848.

Esclusa-Diaz M, Gayo-Otero M, Perez-Marcos M, Vila-Jato J and Torres-Labandeira J (1996). Preparation and evaluation of ketoconazole-β-cyclodextrin multi-component complexes. *Int. J. Pharm.,* **142**(2): 183-187.

Filipović-Grčić J, Voinovich D, Moneghini M, Bećirević-Laćan M, Magarotto L and Jalšenjak I (2000). Chitosan microspheres with hydrocortisone and hydrocortisone–hydroxypropyl-β-cyclodextrin inclusion complex. *Eur. J. Pharm. Sci.,* **9**(4): 373-379.

Furniss BS (1989). Vogel's textbook of practical organic chemistry. *Pearson Education India*.

Kacsó I, Borodi G, Farcas S, Hernanz A and Bratu I. (2010). Host-guest system of Vitamin B10 in β-cyclodextrin: Characterization of the interaction in solution and in solid state. *J. Incl. Phenom. Macrocycl. Chem.,* **68**(1-2): 175-182.

Loftsson T, Hreinsdottir D and Masson M (2005). Evaluation of cyclodextrin solubilization of drugs. *Int. J. Pharm.,* **302**(1-2): 18-28.

Mura P, Adragna E, Rabasco A, Moyano J, Perez-Martinez J, Arias M and Gines J (1999). Effects of the host cavity size and the preparation method on the physicochemical properties of ibuproxam-cyclodextrin systems. *Drug Dev. Ind. Pharm.,* **25**(3): 279-287.

News.vanderbilt.edu. Available online (2010). https://news.vanderbilt.edu. Nanosponge drug delivery system more effective than direct injection.

O'Dowd JJ, Robins DJ and Miller DJ (1988). Detection, characterisation, and quantification of carnosine and other histidyl derivatives in cardiac and skeletal muscle. *Biochim. Biophys. Acta,* **967**(2): 241-249.

Oppermann H, Heinrich M, Birkemeyer C, Meixensberger J and Gaunitz F (2019). The proton-coupled oligopeptide transporters PEPT2, PHT1 and PHT2 mediate the uptake of carnosine in glioblastoma cells. *J. Amino Acids,* **51**(7): 999-1008.

Penjuri SCB, Ravouru N, Damineni S, Bns S and Poreddy SR (2016). Formulation and evaluation of lansoprazole loaded nanosponges. *Turk J. Pharm. Sci.,* **13**(3): 304-310.

Rao M, Bajaj A, Khole I, Munjapara G and Trotta F (2013). *In vitro* and *in vivo* evaluation of b-cyclodextrin-based nanosponges of telmisartan. *J. Incl. Phenom. Macrocycl. Chem.*, **77**(1-4): 135-145.

Sinha V, Chadha R and Goel H (2010). Inter-molecular physiochemical characterization for etodolac-hydroxypropyl-β-cyclodextrin polymeric systems in solid and liquid state. *Open Chemistry,* **8**(4): 953-962.

Spulber M, Pinteala M, Fifere A, Moldoveanu C, Mangalagiu I, Harabagiu V and Simionescu BC (2008). Water soluble complexes of methyl β-cyclodextrin and sulconazole nitrate. *J. Incl. Phenom. Macrocycl. Chem.,* **62**(1-2):135-142.

Swaminathan S, Pastero L, Serpe L, Trotta F, Vavia P, Aquilano D, Trotta M, Zara G and Cavalli R (2010). Cyclodextrin-based nanosponges encapsulating camptothecin: physicochemical characterization, stability and cytotoxicity. *Eur. J. Pharm. Biopharm.,* **74**(2): 193-201.

Swaminathan S, Vavia P, Trotta F and Torne S (2007). Formulation of betacyclodextrin based nanosponges of itraconazole. *J. Incl. Phenom. Macrocycl. Chem.,* **57**(1-4): 89-94.

Tejashri G, Amrita B and Darshana J (2013). Cyclodextrin based nanosponges for pharmaceutical use: A review. *Acta Pharm.,* **63**(3): 335-358.

Terekhova IV and Obukhova NA (2007). Study on inclusion complex formation of m-aminobenzoic acid with native and substituted β-cyclodextrins. *J. Sol. Chem.,* **36**(9): 1167-1176.

Tønnesen HH, Másson M and Loftsson T (2002). Studies of curcumin and curcuminoids. XXVII. Cyclodextrin complexation: Solubility, chemical and photochemical stability. *Int. J. Pharm.,* **244**(1-2):127-135.

Torne S, Darandale S, Vavia P, Trotta F and Cavalli R. (2013). Cyclodextrin-based nanosponges: Effective nanocarrier for Tamoxifen delivery. *Pharm. Dev. Technol.,* **18**(3): 619-625.

Trotta F, Cavalli R, Tumiatti W, Zerbinati O, Roggero C and Vallero R (2007). Ultrasound-assisted synthesis of cyclodextrin-based nanosponges: *Google Patents*, *EP*, **1786841**: A1

Trotta F, Zanetti M and Cavalli R (2012). Cyclodextrin-based nanosponges as drug carriers. *Beilstein J. Org. Chem.,* **8**(1): 2091-2099.